**Proceedings Paper:**
Zhou, Xingwei, Zhao, Xing orcid.org/0000-0003-4000-0446, Liu, Pengxin et al. (1 more author) (2022) A Current Coordinated Optimal Control Strategy for Doubly Salient Electromagnetic Machine. In: 2022 25th International Conference on Electrical Machines and Systems (ICEMS). International Conference on Electrical Machines and Systems, 29 Nov - 02 Dec 2022 IEEE, THA.

https://doi.org/10.1109/ICEMS56177.2022.9983193

# A Current Coordinated Optimal Control Strategy for Doubly Salient Electromagnetic Machine


Xingwei Zhou
College of Energy and Electrical Engineering
Hohai University
Nanjing, China
zhxw@hhu.edu.cn

Peixin Liu
College of Energy and Electrical Engineering
Hohai University
Nanjing, China
211606010045@hhu.edu.cn

Xing Zhao
Department of Electrical Engineering
University of York
York, United Kingdom
xing.zhao@york.ac.uk

Zhao Tian
Jiangsu Port Intelligent Equipment Industry Innovation Center Co., LTD
Nanjing, China
13451929317@163.com

Jinqi Wan
Jiangsu Port Intelligent Equipment Industry Innovation Center Co., LTD
Nanjing, China
117740481@qq.com

Shuangxia Niu
Department of Electrical Engineering
The Hong Kong Polytechnic University
Hong Kong, China
eesxniu@polyu.edu.hk


2022 25th International Conference on Electrical Machines and Systems (ICEMS) | 978-1-6654-9302-4/22/$31.00 ©2022 IEEE | DOI: 10.1109/ICEMS56177.2022.9983193


***Abstract*—The traditional doubly salient electromagnetic machine system sets the filed current to the rated value regardless of load or speed conditions, resulting the problem of large power loss and the limitation of system efficiency. In order to solve this problem, this paper presents a coordinated control strategy of DSEM armature current and field current under multiple working conditions. The loss of DSEM is firstly analyzed, then the loss finite element calculation model is established based ANSYS simulation. The obtained physical quantities are mathematically fitted, and it's utilized for the actual current distribution and coordinated control. High efficient operation over wide ranges of load and speed conditions is desired to be achieved. The simulation and experimental results verify the correctness and feasibility of the proposed method.**


***Keywords—Doubly salient electromagnetic machine, Optimization control strategy , Minimum loss , Current distribution***

## I. INTRODUCTION

The stator and rotor of Doubly Salient Electromagnetic Machine (DSEM) are both of salient pole structure. There's no winding or permanent magnet on the rotor. It has the characteristics of high reliability, flexible magnetic regulation control and strong fault tolerance especially under high-temperature and high-speed conditions. So DSEM has broad application prospects in aviation, new energy power generation and electric vehicles [1-4].

DSEM often operates over wide ranges of speed and load. The traditional DSEM system sets the filed current to the rated value regardless of load or speed conditions, resulting the problem of large power loss and the limitation of system efficiency，especially under light load condition, if the rated field current is adopted, the motor loss will be increased, resulting in low system efficiency [5].

At present, lots of scholars have achieved relavent research results for the current coordination optimization control of motor and the reduction of operating loss. In [6], a simple motor model is used to identify the optimal parameters of the torque distribution function for SRM, and the optimization algorithm of the torque distribution function is summarized to achieve the purpose of maximizing efficiency. This method can effectively improve the motor operation efficiency, but the effect on the field adjustable DSEM is poor. [7] puts forward a new type of DSEM control strategy based on armature current rating and field current regulation, which improves the system efficiency and suppress the cogging torque ripple to a certain extent. However, due to the large field inductance of DSEM, the time constant is large, so only adjusting the field current will affect the dynamic performance of the motor. [8] proposes a method of minimizing the field current increment by controlling the conduction angle to improve the dynamic response characteristics of the motor, which can obtain a fast response of the motor dynamic process by adjusting the field current. But the effect of this method is not obvious in wide speed range, especially in light load condition. [9] cites the penalty function and adopted Lagrange method to propose a control method for minimizing the copper loss of salient pole motor, only the copper loss is considered for the optimization, the influence of iron loss is ignored. In [10], to solve the problem of low efficiency of variable flux vernier reluctance motor, an optimal control strategy for improving full speed operation is proposed based on the D and Q axis coordinate system of synchronous rotation. This method can realize loss minimization control, but it is only applicable to sinusoidal control motor.

Reducing the loss of DSEM under light load is an important problem to be solved. In this paper, a coordinated and optimized control strategy of DSEM armature current and field current under multiple conditions is proposed. The DSEM loss is firstly analyzed in detail, and then the finite element method (FEM) is applied to establish a loss finite element calculation model in ANSYS. The corresponding motor field current and armature current under different speed and torque parameters are simulated, and the obtained physical quantities are mathematically fitted. And then the field current corresponding to the smallest sum of losses is obtained by the traversal algorithm and applied to the control of the DSEM, so as to realize the current distribution and coordinated control. This method can reduce motor losses and improve system operation efficiency in a wide speed and load range. Therefore, the research in this paper has important theoretical and engineering practical significance.

This work was supported by National Natural Science Foundation of China (51907051, 51737006), "Hong Kong Scholar" Program (XJ2021015), China Postdoctoral Science Foundation (2020M671317), the open fund Project of Jiangsu Key Laboratory of Power Transmission & Distribution Equipment Technology (2021JSSPd09), and Jiangsu Province Graduate Student Practice Innovation Program (SJCX22_0181).

## II. The Basic Working Theory of DSEM

Fig. 1 shows the cross-sectional view of a 12/8 pole DSEM, both of the stator and rotor are with salient structure. No armature windings or field windings are mounded the rotor, contributing to its high reliability under harsh working conditions, so is has a promising application for aero power system, wind power generation, *etc*.

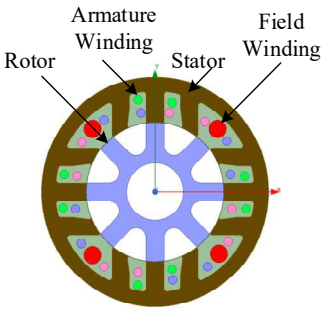


Fig.1. The cross section of the DSEM with the structure of 12/8-pole

Fig. 2 shows the power drive circuit for the DSEM. The armature winding drive uses a three-phase full-bridge inverter, and the field winding control uses an asymmetric half-bridge converter[11]. The two converters are powered by the same DC power supply. There are two parts consisted of the torque $T_p$ of each phase of the DSEM: reluctance torque $T_{pr}$ and field torque $T_{pf}$, of which the field torque is the main component. They are expressed as:

$$T_{pr} = \frac{1}{2} i_p^{\,2} \frac{\partial L_p}{\partial \theta} \tag{1}$$

$$T_{pf} = i_f i_p \frac{\partial L_{pf}}{\partial \theta} \tag{2}$$

Where $T_p$, $i_p$, $L_p$ (p=a, b, c) are three-phase torque, current and inductance, respectively; $L_{pf}$ is the mutual inductance of three-phase windings and field windings.

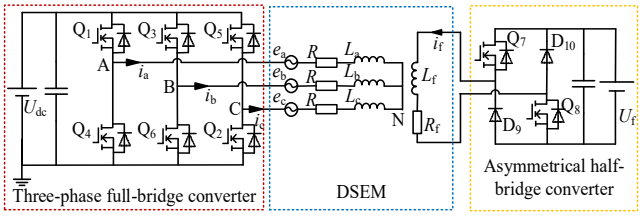


Fig.2. Main power circuits for DSEM driving

Fig. 3 shows the three-phase inductance curves and the general conduction rule of DSEM. Positive current is conducted to the inductor rising area, while negative current conducts through the inductor falling area. In order to ensure the stable operation of the electric cycle, three commutation instants should be detected in time.

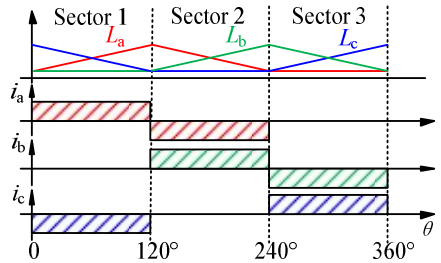


Fig.3. "120° three step" conduction mode

## III. Loss Analysis And Finite Element Simulation of DSEM

### A. Loss analysis of DSEM

Fig. 4 shows the loss flow diagram of the DSEM. $P_s$ and $P_t$ are the loss of the power devices of the system inverter, and this part of the loss is reduced mainly by updating the devices and improving the modulation strategy. $P_m$ and $P_z$ are the mechanical loss and stray loss, respectively, which are reduced mainly by improving the motor structure, so they are usually not involved in the study of control strategies. The main losses in the operation of the motor are iron loss $P_{fe}$ and copper loss $P_{cu}$, and for the motor that have been designed and used, this part of the loss can be reduced by improving the control strategy, so this paper analyzes the iron loss and copper loss of the motor at first.

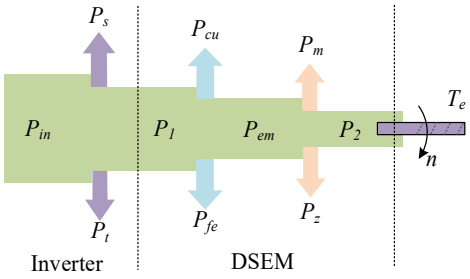


Fig.4. Loss flow diagram of DSEM

The copper loss of DSEM can be expressed as:

$$P_{cu} = P_{cup} + P_{cuf} = k_p i_p^2 R_p + i_F^2 R_F \tag{3}$$

The iron loss is made up of hysteresis loss, eddy current loss, and additional loss, and a three-term loss separation model can be established [12]. In further, the binomial model considering the additional loss as a part of the eddy current loss is proposed [13]. This paper analyzes the power of DSEM based on the above theories, the expression of $P_{Fe}$ can be obtained.

$$p_{Fe} = p_h + p_c = k_h B_m^2 f + k_c (B_m f)^2 \tag{4}$$

However, the hysteresis loss coefficient $k_h$ and eddy current loss coefficient $k_c$ of ferromagnetic materials will vary with the change of physical quantities such as magnetization frequency and magnetic density amplitude, it is difficult to obtain online. So when calculating the iron loss, the magnetic density amplitude is simplified and analyzed according to the average method.

$$P_{Fe} = P_h + P_c = k_h f (\frac{B_{\max} - B_{\min}}{2})^2 + k_c f^2 (\frac{B_{\max} - B_{\min}}{2})^2 \tag{5}$$

The relationship between the motor magnetic density and the magnetic chain is as shown in equation (6), ignoring the self-inductive change of the three phases of the motor, and the definition of the magnetic chain is shown in equation (7):

$$B = k_\varphi \psi \tag{6}$$

$$\psi = i_F L_{pF} \tag{7}$$

Combining (5), (6), (7), formula (8) can be obtained.

$$P_{Fe} = P_h + P_c = k_h \cdot f \cdot \frac{i_F^{\,2} (L_{pF\max} - L_{pF\min})^2}{4} + k_c \cdot f^2 \cdot \frac{i_F^{\,2} (L_{pF\max} - L_{pF\min})^2}{4} \tag{8}$$

So a model of iron los for DSEM can be achieved, as shown in formula (9).

$$P_{Fe} = k_1 \omega {i_F}^2 + k_2 \omega^2 {i_F}^2 \tag{9}$$

In summary, the expression of the sum of iron loss and copper loss during DSEM operation can be obtained as follows:

$$\begin{aligned} P_{Loss} &= P_{Cu} + P_{Fe} \\ &= k_p i_p^2 R_p + i_F^2 R_F + k_1 \omega {i_F}^2 + k_2 \omega^2 {i_F}^2 \end{aligned} \tag{10}$$

Where $k_p$=2, $k_1 = k_h \cdot \frac{(L_{pF\max} - L_{pF\min})^2}{4 \cdot 2\pi}$, $k_2 = k_c \cdot \frac{(L_{pF\max} - L_{pF\min})^2}{4 \cdot 2\pi}$.

Under the aforementioned condition of ignoring the motor reluctance torque [14], the output torque of the motor can be expressed as:

$$T_e = 2T_p = 2 i_F i_p \frac{\partial L_{pF}}{\partial \theta} = C_t(i_F, i_p) i_F i_p \tag{11}$$

Where $C_t$ is the torque coefficient of the motor.

Using the Lagrange multiplier method, the minimum loss field current under the current working conditions is obtained according to the torque and speed of the motor:

$$i_F = \sqrt[4]{\frac{2 {T_e}^2 R_p}{C_t(i_F, i_p)^2 (k_1 \omega + k_2 \omega^2 + R_F)}} \tag{12}$$

### *B. Finite element simulation analysis and parameter fitting*

In order to obtain the parameters in formula (12), the iron loss should be accurately calculated, in this paper, it's obtained through ANSYS FEM simulation. Firstly, the stator and rotor of the motor are divided into several micro elements, and the electromagnetic field of the motor is analyzed by FEM, and the magnetic density change curve at the midpoint of each micro element is obtained. The ferromagnetic loss of each micro element is calculated according to the calculation model of ferromagnetic materials, and then the sum is the total iron loss of the motor [15]. Meanwhile, the simulation can obtain physical quantities such as torque and loss under the combination of field current and armature current at different speeds. The relationship between the obtained electromagnetic torque coefficient $C_t$ and the field current and armature current is shown in Figs. 5 and 6. Among them, Fig. 6 shows the fitting curve of electromagnetic torque coefficient $C_t$ and armature current $i_p$ under five conditions of $i_F$ = 2M (M = 1, 2,... 5).

From Fig. 5 and Fig. 6, the relationship between the electromagnetic torque coefficient and the field current and armature current can be concluded as follows: the electromagnetic torque coefficient shows a weak correlation with the armature current, and its change trend is mainly determined by the change of field current. The main reason for the analysis is that the field inductance of DSEM is much greater than the self-inductance of the armature, so the field torque component of the motor is much greater than the reluctance torque component. Considering the influence of magnetic field saturation of the motor, it can be approximated that the electromagnetic torque coefficient $C_t$ can be expressed by the field current $i_F$ piecewise linearly.

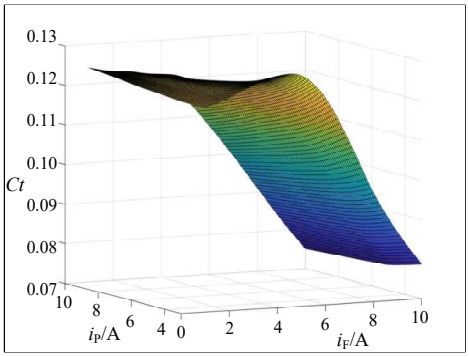


Fig.5. Relationship between electromagnetic torque coefficient $C_t$ with $i_F$ and $i_p$

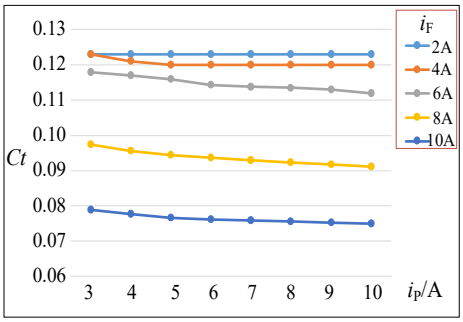


Fig.6. Relationship between electromagnetic torque coefficient $C_t$ with $i_p$

Using the sum of iron loss and copper loss obtained by simulation under different speeds, field currents, and armature current combinations as a reference value, according to equation (10), the values of parameters $k_1$ and $k_2$ are obtained by using the least squares method.

In summary, based on the ANSYS finite element simulation and calculation, the values of the electromagnetic torque coefficient $C_t(i_F)$ and the parameters $k_1$ and $k_2$ are obtained, so the field current distribution value that satisfies the sum of the motor operating losses under any one working condition can be calculated, and then the current coordination and optimization control can be practiced, which can reduce the motor loss in a wide speed load range and improve the system operation efficiency.

Table I shows the simulation results at 1000rpm and 3.4Nm of DSEM in ANSYS. The loss under the coordinated optimization control strategy is smaller than that of the traditional control strategy.

TABLE I. Finite element simulation results

| ***Control strategy*** | ***$i_F$*/A** | ***$i_p$*/A** | **Loss/W** |
|---|---|---|---|
| *Traditional control* | 6 | 5 | 88.64 |
| *Coordinated optimization control* | 4.6 | 6.5 | 82.23 |

Fig. 7 and Fig. 8 show the DSEM magnetic density simulation diagram under the traditional control strategy and the current coordination optimization control strategy, respectively. When the mechanical angle is 0°, the magnetic density of the motor under the traditional control strategy is significantly greater than that of the current coordination optimization control strategy. When the motor is rotated to a mechanical angle of 15°, the magnetic density of the coordinated optimization control strategy is also smaller than that of traditional control. Simulation results show that the proposed optimal control strategy can reduce motor loss and improve operation efficiency.

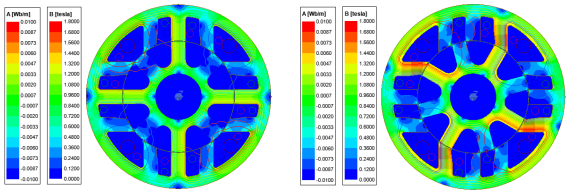

(a) 0° (b) 15°

Fig.7. Simulation diagram of DSEM magnetic density of traditional method

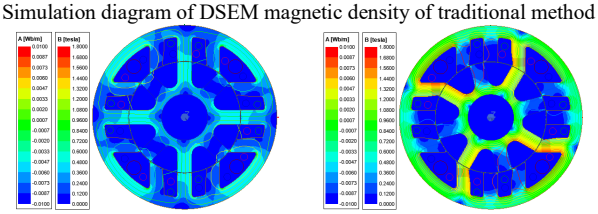

(a) 0° (b) 15°

Fig.8. Simulation diagram of DSEM magnetic density of Current coordination optimization method

## IV. Coordinated Optimal Control Method of Field Current And Armature Current

The traditional DSEM system sets the field current to the rated value regardless of load or speed conditions, resulting in the problem of large power loss and the limitation of system efficiency. In order to solve this problem, this paper presents a coordinated control strategy of DSEM armature current and field current under multiple working conditions. It avoids complex iron loss calculations while enabling efficient operation of the motor over a wide speed load range.

The key to the current coordinated optimization control strategy proposed in this paper lies in:

*1)* The torque of the motor should be accurately calculated. Due to the slow update rate of the platform torque sensor, it cannot be applied to the control system. In this paper, the field current and armature current are sampled to calculate the accurate torque value of the motor operation through the torque observer.

*2)* The motor losses are precisely acquired. Since the iron loss parameters of the motor are difficult to be obtained or calculated online, the loss model is established in ANSYS, and the motor loss data under different working conditions is obtained by offline calculation.

*3)* The given value of the current is traversed in real time. This paper shortens the program execution time by programming the frequency adjustment to ensure the accuracy of the calculation, so that the results obtained by the traversal are consistent with the parameters of the current operating conditions, so as to achieve accurate traversal of a given current.

The proposed control strategy diagram shown in Fig. 9 is utilized to optimize the control of current coordination by distributing the least field current between the sum of iron loss and copper loss. The main circuit part of DSEM is a double closed-loop structure with speed and armature current. The output of the current closed loop is connected to a PI regulator. The drive signal of the full-bridge converter is then generated. The field circuit obtains the torque of the motor operation through the torque observer. Using the traversal algorithm and combining the real-time speed, the iron loss and copper loss values under different field currents are calculated, and then the output of the field current at the minimum loss is used as a given value to form a closed loop of the field current. And the field current output generates the drive signal of the asymmetric half-bridge converter through the PI regulator.

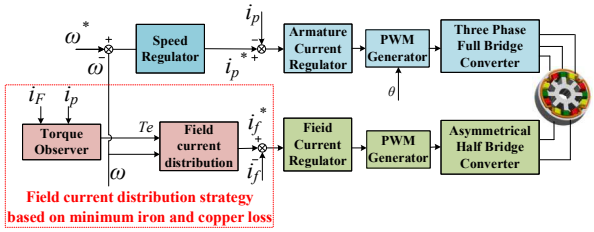


Fig.9. DSEM current coordination control strategy diagram

The specific distribution process of field current is shown in Fig. 10. First of all, the finite element loss calculation model is built in ANSYS, the iron loss and copper loss of the DSEM under different torque and speed conditions are obtained, and the obtained physical quantities are mathematically fitted. Then, combined with the torque and speed of the motor operation, the field current is traversed and calculated over the range of 0-10A according to the 0.1A interval, and the field current with the smallest sum of losses is obtained as a given value output to form a closed loop of field current.

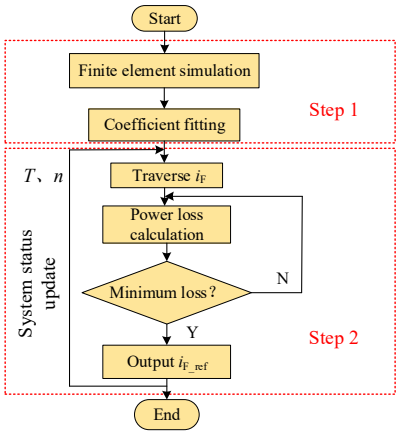


Fig. 10. Flow chart of field current distribution

## V. Experimental Results

Fig. 11 shows the DSEM experimental prototype platform. It mainly contains a 12/8 pole three-phase DSEM, three-phase full-bridge inverter circuit, permanent magnet synchronous motor coaxially connected to DSEM, sampling and driving circuit, adjustable ohmic load, *etc*. When the system operates, DSEM acts as a motor to drag the coaxial PMSM rotation power generation, connects the adjustable ohmic load through the rectifier bridge.

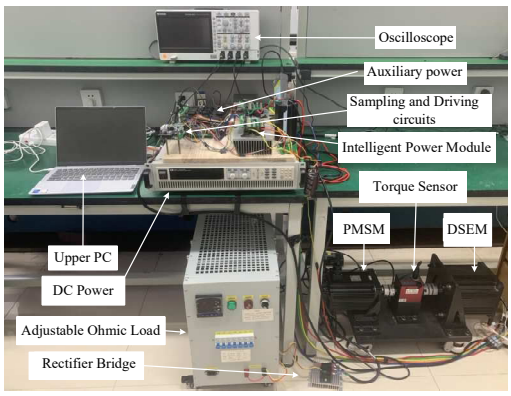


Fig. 11. Experimental prototype

Fig. 12 shows the comparison diagram of current experiment between traditional control strategy and optimized control strategy under no-load condition at 1000 rpm. Fig. 13 shows the comparison diagram of 600 rpm and 48 Ω loading.

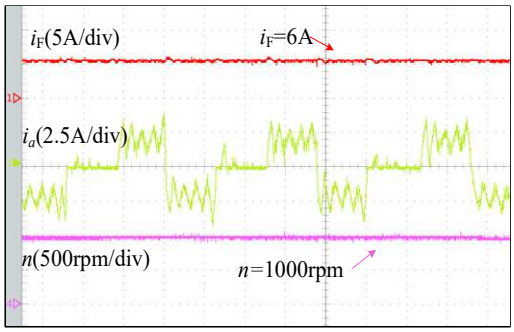


T/(2ms/div)

(a) Traditional method

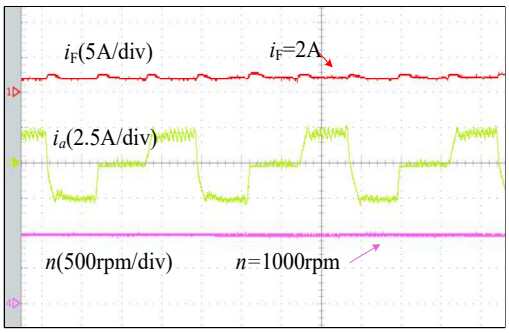


T/(2ms/div)

(b) Proposed method

Fig. 12. Experimental comparison diagram of R = ∞

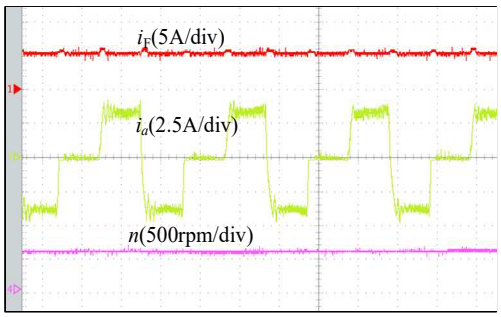


T/(4ms/div)

(a) Traditional method

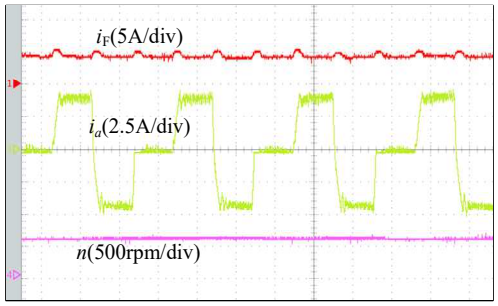


T/(4ms/div)

(b) Proposed method

Fig. 13. Experimental comparison result of R = 48Ω

Fig. 14 shows the experimental comparison of the DC bus currents obtained by the two strategies under different operating conditions. Due to the accuracy limitation of torque sensor, this paper analyzes the power loss through the DC bus current from DC power display. The results show that the DC bus current of the current coordination optimization control strategy is significantly lower than that of the traditional control strategy, that is, the motor loss is more smaller.

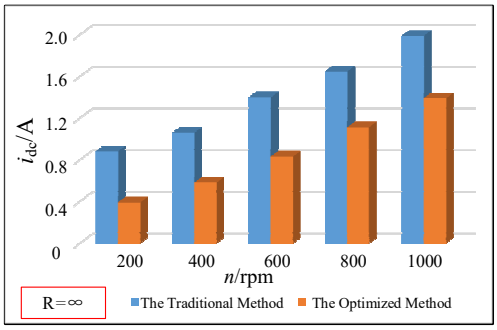


(a) R=∞

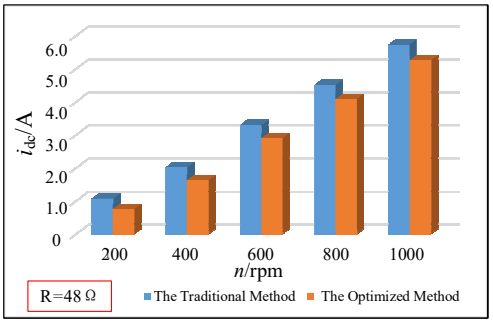


(b) R=48Ω

Fig. 14. The comparison diagram of DC bus current under different working conditions of two strategies

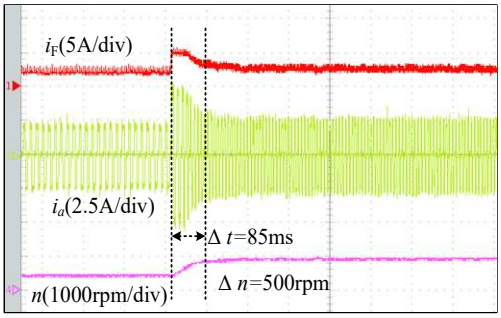


T(100ms/div)

(a) Accelerate

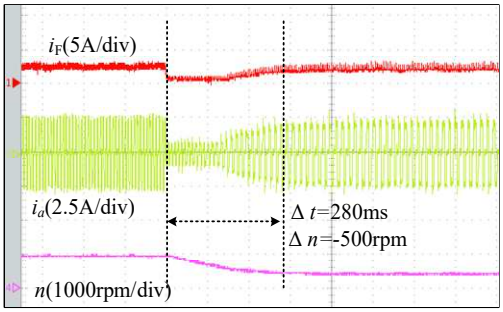


T/(100ms/div)

(b) Decelerate

Fig. 15. The dynamic acceleration and deceleration experimental results

Fig. 15 shows the experimental results of motor acceleration and deceleration under the coordinated

optimization control strategy, and the experimental results show that the strategy has good dynamic effect, which can achieve stable operation of the DSEM.

## VI. Conclusions

Large power loss is caused by the rated filed current under the traditional DSEM control strategy. To overcome this problem, the DSEM power loss is analyzed in this paper, based on the FEM simulation results and power loss fitting calculation method, a coordinated optimization control method of field current and armature current is proposed, it can improve the system efficiency over wide ranges of load and speed condition. The effectiveness of the proposed method is verified by multifarious experiments.

## References


[1] Z. Chen, B. Wang, Z. Chen et al, "Comparison of Flux Regulation Ability of the Hybrid Field Doubly Salient Machines," *IEEE Trans. Ind. Electron*., vol.61, no. 7, pp.3155-3166, July. 2014.

[2] X. Zhou, B. Zhou, J. Yu et al, "Research on Initial Rotor Position Estimation and Anti-Reverse Startup Methods for DSEM," *IEEE Trans. Ind. Electron*., vol. 64, no. 4, pp.3297-3307, April, 2017.

[3] Z. Zhang, L. Yu, L. Sun, et al, "Iron Loss Analysis of Doubly Salient Brushless DC Generators," *IEEE Trans. Ind. Electron*., vol.62, no.4, pp.2156-2163, Apr. 2015.

[4] X. Liu and Z. Q. Zhu, "Comparative Study of Novel Variable Flux Reluctance Machines With Doubly Fed Doubly Salient Machines," *IEEE Trans. Magn.*, vol. 49, no. 7, pp. 3838-3841, July 2013.

[5] W. Jia, L. Xiao and D. Zhu, "Core-Loss Analysis of High-Speed Doubly Salient Electromagnetic Machine for Aeronautic Starter/Generator Application," *IEEE Trans. Ind. Electron*., vol. 67, no. 1, pp.59-68, Jan. 2020.

[6] V. P. Vujičić, "Minimization of Torque Ripple and Copper Losses in Switched Reluctance Drive," *IEEE Trans. Power Electron*., vol. 27, no. 1, pp. 388-399, Jan. 2012.

[7] X. Zhou, L. Zhang and F. Wu, "Operating Performance Enhancing Method for Doubly Salient Electromagnetic Machine Under Light Load Condition," *IEEE Access,* vol. 8, pp. 112057-112065, 2020.

[8] K. Wang, B. Zhou, X. Zhou, J. Wei and Z. Zhou, "Minimum Field Current Increment Control for Doubly Salient Electro-Magnetic Generator With Improved Dynamic Performance," *IEEE Trans. Ind. Electron*, vol. 69, no. 5, pp. 4566-4575, May 2022.

[9] Zhao J, Lin M, Xu D, "Minimum-copper-loss control of hybrid excited axial field flux-switching machine," *IET Electr. Power Appl*., vol. 10, no. 2, pp. 82-90, 2016.

[10] H. Lu, J. Li, R. Qu and S. Jia, "Loss minimization control of vernier reluctance machines with DC field windings in stator," IECON 2015 - 41st Annual Conference of the IEEE Industrial Electronics Society, 2015, pp. 001885-001890.

[11] S. Jiang, B. Zhou, X. Huang, K. Wang and L. Xu, "3-D Global Thermal Analysis of DSEM Considering the Temperature Difference Between Field and Armature Coils," *IEEE Trans. Ind. Electron*., vol. 68, no. 12, pp. 11931-11940, Dec. 2021.

[12] G. Bertotti, "General properties of power losses in soft ferromagnetic materials," *IEEE Trans. Magn.*, vol. 24, no. 1, pp. 621-630, Jan. 1988.

[13] Q. Yu, B. Bilgin and A. Emadi, "Loss and Efficiency Analysis of Switched Reluctance Machines Using a New Calculation Method," *IEEE Trans. Ind. Electron.*, vol. 62, no. 5, pp. 3072-3080, May 2015.

[14] X. Zhou, B. Zhou and K. Wang, "Position Sensorless Control for Doubly Salient Electromagnetic Machine With Improved Startup Performance," *IEEE Trans. Ind. Electron*., vol. 67, no. 3, pp. 1782-1791, March 2020.

[15] W. Jia, L. Xiao, D. Zhu and J. Wei, "An Improved Core-Loss Calculation Method With Variable Coefficients Based on Equivalent Frequency," *IEEE Trans. Magn.*, vol. 54, no. 11, pp. 1-5, Nov. 2018.